The Plant Cell, Vol. 25: 1726–1739, May 2013, www.plantcell.org

The α/β Hydrolase CGI-58 and Peroxisomal Transport Protein PXA1 Coregulate Lipid Homeostasis and Signaling in *Arabidopsis*[W]

Sunjung Park,[a,b,1] Satinder K. Gidda,[c,1] Christopher N. James,[b,1] Patrick J. Horn,[b] Nicholas Khuu,[c] Damien C. Seay,[a,2] Jantana Keereetaweep,[b] Kent D. Chapman,[b] Robert T. Mullen,[c,3] and John M. Dyer[a,3,4]

[a] U.S. Department of Agriculture–Agricultural Research Service, U.S. Arid-Land Agricultural Research Center, Maricopa, Arizona 85138

[b] Department of Biological Sciences, Center for Plant Lipid Research, University of North Texas, Denton, Texas 76203

[c] Department of Molecular and Cellular Biology, University of Guelph, Guelph, Ontario, Canada N1G 2W1

COMPARATIVE GENE IDENTIFICATION-58 (CGI-58) is a key regulator of lipid metabolism and signaling in mammals, but its underlying mechanisms are unclear. Disruption of *CGI-58* in either mammals or plants results in a significant increase in triacylglycerol (TAG), suggesting that CGI-58 activity is evolutionarily conserved. However, plants lack proteins that are important for CGI-58 activity in mammals. Here, we demonstrate that CGI-58 functions by interacting with the PEROXISOMAL ABC-TRANSPORTER1 (PXA1), a protein that transports a variety of substrates into peroxisomes for their subsequent metabolism by β-oxidation, including fatty acids and lipophilic hormone precursors of the jasmonate and auxin biosynthetic pathways. We also show that mutant *cgi-58* plants display changes in jasmonate biosynthesis, auxin signaling, and lipid metabolism consistent with reduced PXA1 activity in planta and that, based on the double mutant *cgi-58 pxa1*, *PXA1* is epistatic to *CGI-58* in all of these processes. However, *CGI-58* was not required for the PXA1-dependent breakdown of TAG in germinated seeds. Collectively, the results reveal that CGI-58 positively regulates many aspects of PXA1 activity in plants and that these two proteins function to coregulate lipid metabolism and signaling, particularly in nonseed vegetative tissues. Similarities and differences of CGI-58 activity in plants versus animals are discussed.

INTRODUCTION

COMPARATIVE GENE IDENTIFICATION-58 (*CGI-58*) encodes an α/β hydrolase–type protein that plays a key role in regulating triacylglycerol (TAG) homeostasis in both mammals and plants (James et al., 2010; Radner et al., 2011). In humans, mutations of *CGI-58* cause Chanarin-Dorfman syndrome, a rare neutral lipid storage disorder characterized by an increase in lipid droplets (LDs) in cell types that do not normally store lipids, such as liver, skin, skeletal muscle, and blood cells (Lefèvre et al., 2001). CGI-58 is a soluble protein that is conditionally localized to the surface of LDs in mammalian cells via protein–protein interaction with an LD-associated protein called perilipin (Yamaguchi et al., 2004). Upon adrenergic stimulation, perilipin becomes phosphorylated, which releases CGI-58 from perilipin and allows it to interact with and stimulate the activity of adipose triglyceride lipase (ATGL), which subsequently degrades TAG to produce fatty acids (FAs) (Subramanian et al., 2004; Lass et al., 2006). Loss of CGI-58 activity is therefore thought to result in aberrant TAG turnover, resulting in enhanced TAG accumulation in LDs.

However, there are many aspects of CGI-58 function in mammals that are poorly understood. Disruption of *CGI-58* not only results in an increase in TAG, but also promotes an increase in diacylglycerol, ceramides, and phosphatidylglycerol, as well as changes in the composition of the phospholipid pool (Igal and Coleman, 1996; Brown et al., 2010). In addition, despite an increase of TAG in non-lipid-storing cell types, knockdown of *CGI-58* in mice unexpectedly appears to improve both systemic insulin sensitivity and protection from high-fat-induced obesity (Brown et al., 2010). Loss of CGI-58 activity in mice also resulted in a reduction of PPARα-dependent gene expression, suggesting that CGI-58 is somehow involved in generating or regulating lipid signals required for the activation of this transcription factor (Brown et al., 2010). Mammalian CGI-58 also was shown to have lysophosphatidic acid acyltransferase (LPAAT) activity in vitro (Ghosh et al., 2008; Montero-Moran et al., 2010), and this activity recently was associated with the production of phosphatidic acid (PA) in vivo as a second messenger during tumor necrosis factor signaling (Lord et al., 2012). These and other observations indicate that CGI-58 acts as a central regulator that integrates energy, Glc, and TAG homeostasis with adipogenesis and inflammatory responses in mammals and that CGI-58 has ATGL-independent activities that potentially include interaction with other proteins, inherent enzyme activity, and the production of as yet unknown lipid signals.

[1] These authors contributed equally to this work.

[2] Current address: Department of Natural Sciences, Del Mar College, Corpus Christi, TX 78404.

[3] These authors contributed equally to this work.

[4] Address correspondence to john.dyer@ars.usda.gov.

The authors responsible for distribution of materials integral to the findings presented in this article in accordance with the policy described in the Instructions for Authors (www.plantcell.org) are: Robert T. Mullen (rtmullen@uoguelph.ca) and John M. Dyer (john.dyer@ars.usda.gov).

[W] Online version contains Web-only data.

www.plantcell.org/cgi/doi/10.1105/tpc.113.111898

Loss of CGI-58 activity in plants similarly results in accumulation of TAG in cell types that do not normally accumulate lipid, such as leaf mesophyll cells, as well as changes in membrane lipid content and composition, including both phospholipids and galactolipids (James et al., 2010). The accumulation of TAG in both plants and mammals suggests that some aspects of CGI-58 function are evolutionarily conserved, but plants lack any apparent homologs to perilipin (Chapman et al., 2012). Thus, based on the importance of protein–protein interactions in the function of CGI-58 in mammals, we employed a yeast two-hybrid approach to identify *Arabidopsis thaliana* CGI-58–interacting proteins in plants. One of the candidate CGI-58–interacting proteins identified through this screen was PEROXISOMAL ABC-TRANSPORTER1 (PXA1), a peroxisomal membrane protein that plays multiple essential roles in plant lipid metabolism and signaling (Zolman et al., 2001; Footitt et al., 2002; Hayashi et al., 2002; Theodoulou et al., 2005). Using a combination of genetic, biochemical, and physiological experiments, we show that CGI-58 positively regulates many aspects of PXA1 function in plant cells, particularly in the turnover of polyunsaturated FAs and the metabolism of lipid hormone precursors, including compounds of the jasmonate and auxin biosynthetic pathways. Overall, these results have broad implications for understanding novel aspects of lipid homeostasis and lipophilic signaling in plants and potentially illuminate new functions for CGI-58 in energy maintenance and lipid signaling in other eukaryotes.

RESULTS

CGI-58 Interacts with the C-Terminal Walker B Motif of Peroxisomal PXA1

To gain insight to the molecular function of CGI-58 in plants, we screened an *Arabidopsis* cDNA library using CGI-58 as bait in a yeast two-hybrid system and identified three strongly interacting proteins (see Supplemental Table 1 and Supplemental Figure 1 online). Sequencing of the respective prey plasmids revealed that one of the interacting proteins contained a polypeptide sequence corresponding to the C-terminal 142 amino acids of the peroxisomal transport protein PXA1. PXA1 is known to play a number of important roles in plant lipid metabolism, including the transport of FAs into peroxisomes for breakdown by β-oxidation as well as uptake of several lipophilic hormone precursors, including 12-oxophytodienoic acid (OPDA) and indole-3-butyric acid (IBA), for their subsequent conversion via β-oxidation into biologically more active forms, namely, jasmonic acid (JA) and indole-3-acetic acid (IAA), respectively (Figure 1) (Zolman et al., 2001; Footitt et al., 2002; Hayashi et al., 2002; Theodoulou et al., 2005; Eastmond, 2006; Dave et al., 2011). Moreover, disruption of *PXA1* was previously shown to result in elevated accumulation of LDs and TAG in vegetative tissues under certain physiological conditions (Kunz et al., 2009; Slocombe et al., 2009). The general similarity of oil accumulation phenotypes in both *cgi-58* (James et al., 2010) and *pxa1* mutant (Kunz et al., 2009; Slocombe et al., 2009) plants suggested that CGI-58 and PXA1 might function cooperatively in regulating lipid metabolism and signaling; thus, the relationships between CGI-58 and PXA1 were investigated further.

PXA1 is a full-size ABC transport protein that consists of two duplicated regions, each of which contains six putative membrane-spanning domains followed by a cytosol-exposed nucleotide binding domain (NBD) composed of Walker A and B motifs (Figure 2A; see Supplemental Figure 2 online for the polypeptide sequence of PXA1). The fragment of PXA1 identified in the yeast two-hybrid screen included the Walker B motif of the second NBD (NBD2-B) (Figures 2B and 2C), which is a region known to be important for regulating the activity of PXA1 in planta (Dietrich et al., 2009; Zolman et al., 2001). Although we were unable to detect an interaction between CGI-58 and full-length PXA1 expressed in yeast cells using the two-hybrid assay, CGI-58 could pull down full-length PXA1 protein in coimmunoprecipitation assays in vitro (Figure 2D; see Supplemental Figure 3 online). As such, additional experiments were conducted to further characterize the interaction between CGI-58 and the C-terminal region of PXA1. For instance, CGI-58 also was able to bind in the yeast two-hybrid assay to the entire NBD2 region containing both Walker A and B motifs (Figures 2B and 2C). However, CGI-58 did not bind the NBD2-A region alone or to any region of NBD1

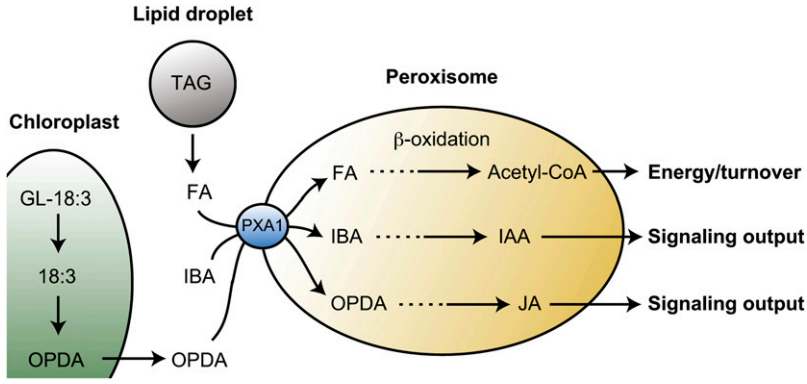

Figure 1. Model for PXA1 Activity in Plant Cells.

PXA1 is required for uptake of FAs from LDs (and other cellular sources) for β-oxidation, import of IBA for conversion to the auxin hormone IAA, and import of OPDA into peroxisomes for conversion to JA. GL-18:3, galactolipid containing 18:3. See text for additional details.

(Figures 2B and 2C). CGI-58 also did not bind to a mutant version of NBD2-B where the sequence was changed to match that of the *pxa1* mutant, where the C-terminal 31 amino acids of the PXA1 protein is replaced with a different sequence of 19 amino acids due to a splice site mutation, and which severely disrupts PXA1 activity in plants (Dietrich et al., 2009; Zolman et al., 2001) (Figures 2B and 2C, and Supplemental Figure 2 online). By contrast, the introduction of a point mutation into the NBD2-B sequence ($D_{1276}\Delta N$), which has only a mild effect on PXA1 activity in vivo (Dietrich et al., 2009) and no detectable effect in vitro (De Marcos Lousa et al., 2009), did not prevent interaction with CGI-58 (Figures 2B and 2C).

The interaction of CGI-58 and the NBD2-B region of PXA1 also was supported by results from a complementary series of nuclear relocalization assays in plant suspension-cultured cells (Figures 2B and 2E), whereby a green fluorescent protein (GFP)–tagged version of CGI-58 was coexpressed with various regions of PXA1 fused to the red fluorescent protein and a nuclear localization signal (RFP-NLS). While coexpression of GFP-CGI-58 and RFP-NLS resulted in the cytosolic localization of GFP-CGI-58 and nuclear localization of RFP-NLS, as expected (Dhanoa et al., 2010; James et al., 2010) (Figure 2E, top row of images), coexpression of GFP-CGI-58 with RFP-NLS fused to the PXA1 NBD2-B region resulted in a portion of GFP-CGI-58 being relocalized to the nucleus due to protein–protein associations (white arrowhead in second row of images in Figure 2E). Similar nuclear relocalization was observed when GFP-CGI-58 was coexpressed with RFP-NLS fused to the NDB2-B region harboring the minor $D_{1276}\Delta N$ mutation (Figure 2E, fourth row) but not when RFP-NLS was fused to the NBD2-B region containing the more extensive *pxa1* mutation at the C terminus (Figure 2E, third row). Taken together, the results presented in Figure 2 demonstrate that CGI-58 interacts specifically with the C-terminal NBD2-B region of PXA1 and that mutations in this sequence that are known to modulate the activity of PXA1 in vivo similarly modulate its interaction with CGI-58.

CGI-58 Localizes to the Surface of Peroxisomes in Plant Cells

The results presented in Figure 2E and in our earlier studies (James et al., 2010) indicate that CGI-58 is localized primarily to the cytosol in plant cells when analyzed in transient expression assays and at early time points. On the other hand, the observation that CGI-58 interacts with the C-terminal region of PXA1, which is oriented toward the cytosol in the context of the full-length protein (Figure 2A) (Nyathi et al., 2010), implies that CGI-58 might localize also to peroxisomes. Indeed, as shown in Figure 3 (top row), transient expression of GFP-CGI-58 in tobacco (*Nicotiana tabacum*) leaves using *Agrobacterium tumefaciens* infiltration revealed that at early time points after infection (i.e., 2 d) the protein localized primarily to the cytosol but also was associated with peroxisomes that were labeled with the coexpressed peroxisomal matrix marker Cherry-PTS1 (Ching et al., 2012). At later times points after infection (i.e., 4 or 5 d), the majority of GFP-CGI-58 was associated with peroxisomes (Figure 3, middle row). In fact, peroxisomal-associated GFP-CGI-58 often exhibited a ring-like fluorescence pattern that surrounded the Cherry-PTS1–labeled peroxisomal matrix (Figure 3, bottom row), suggesting that CGI-58 was localized to the cytosolic surface of the peroxisomal boundary membrane. A similar peroxisomal membrane ring-like fluorescence pattern was observed when GFP-CGI-58 was expressed in the absence of Cherry-PTS1 but not when GFP alone was coexpressed with Cherry-PTS1 (see Supplemental Figure 4 online).

CGI-58 and PXA1 Genetically Interact and Coregulate JA Signaling during Stress Response in Plants

Our working hypothesis is that CGI-58 functions, at least in part, by positively regulating the transport activity of PXA1. To test this hypothesis, we analyzed wild-type, *cgi-58*, *pxa1*, or *cgi-58 pxa1* mutant *Arabidopsis* plants in a variety of physiological assays known to be dependent on PXA1 transport activity. First, mechanical wounding of wild-type plants induces the production of JA, whose synthesis is believed by most to begin with the release of linolenic acid from galactolipids in the plastid, followed by a series of metabolic transformations that eventually produce OPDA (Figure 1) (Gfeller et al., 2010). OPDA is transported into peroxisomes via PXA1 and converted to JA (Theodoulou et al., 2005; Dave et al., 2011). In plants disrupted in *pxa1*, the amount of wound-inducible JA was significantly reduced compared with the wild type, consistent with a reduction in OPDA uptake by PXA1 (Figure 4A) (Theodoulou et al., 2005). *cgi-58* mutant plants also displayed a reduction in wound-inducible JA formation compared with the wild type, although the phenotype was perhaps not as severe as in the *pxa1* mutant (Figure 4A). On the other hand, the *cgi-58 pxa1* double mutant displayed a phenotype that was similar to *pxa1* alone (Figure 4A), indicating that *PXA1* was epistatic to *CGI-58* in these assays and consistent with the hypothesis that CGI-58 functions in part by modulating the activity of PXA1.

Measurement of gene expression patterns in the mechanically wounded *Arabidopsis* plants using quantitative RT-PCR (qRT-PCR) provided further insight to the functional relationships of *CGI-58* and *PXA1* during stress response. For instance, *CGI-58* expression was stimulated ~10-fold in wild-type plants in response to wounding, but this increase was reduced by half in *pxa1* mutant plants (Figure 4B). Similarly, the expression of allene oxide synthase (*AOS*), a wound-inducible gene involved in metabolic transformation of linolenic acid into OPDA in the plastids (Gfeller et al., 2010), also was reduced moderately in both *pxa1* and *cgi-58* plants and was reduced significantly in the *cgi-58 pxa1* double mutant plants (Figure 3B). These results indicate that *CGI-58* is induced during the plant wounding response, that this induction is dependent partially on *PXA1*, and that both *CGI-58* and *PXA1* likely participate in amplifying the stress-induced JA signaling pathway through feedback regulation at the transcriptional level.

CGI-58 and PXA1 Participate in the Physiological Response to Auxins

PXA1 also is required for the transport of the auxin IBA into peroxisomes for its subsequent conversion to IAA, which is a potent regulator of plant growth and development (Figure 1) (Zolman et al., 2001; Hayashi et al., 2002). Inclusion of either IBA

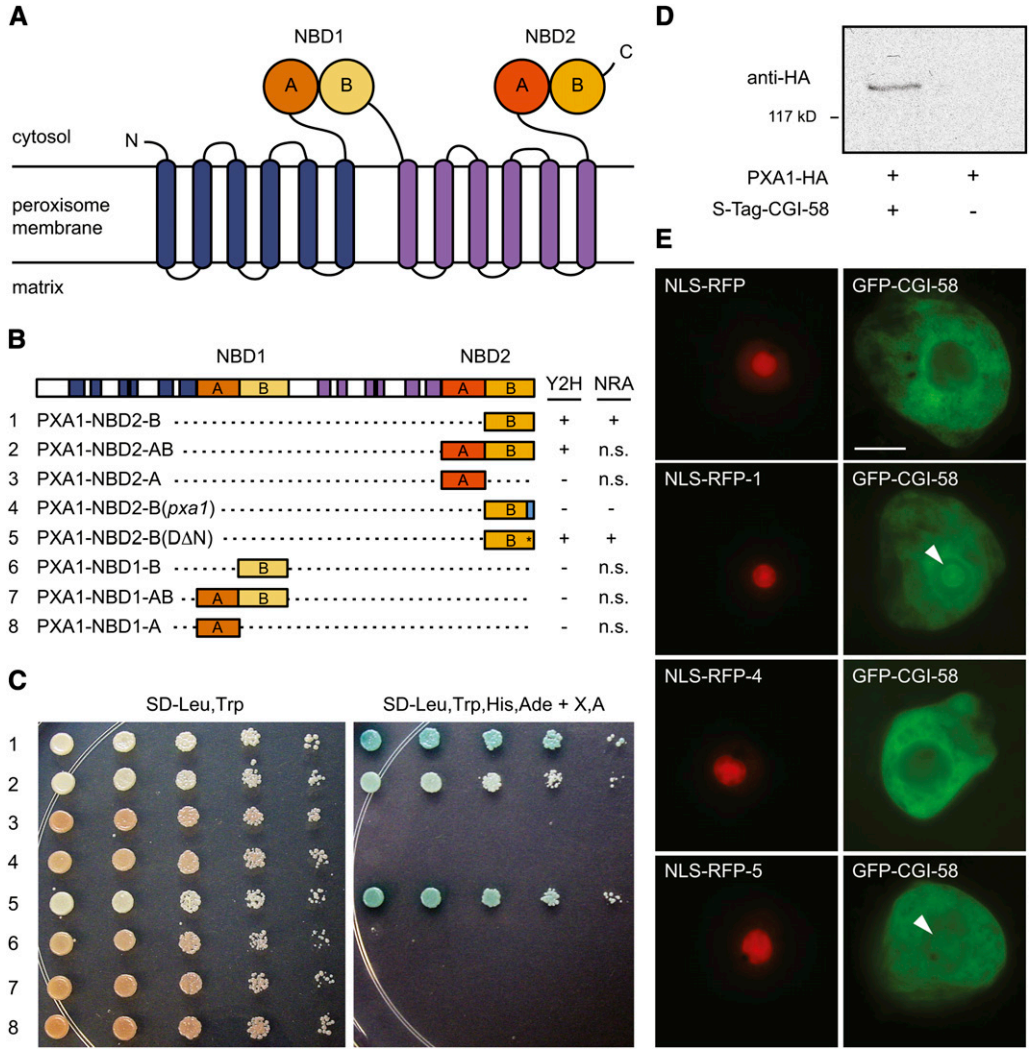

Figure 2. Interaction of CGI-58 with Various Regions of PXA1.

(A) Cartoon of PXA1 structure and topology showing peroxisomal membrane-associated regions and two NBDs, each composed of Walker A and B motifs.
(B) Summary of yeast two-hybrid (Y2H; **[C]**) and nuclear relocalization (NRA; **[E]**) assays, where CGI-58 was tested for its ability to interact with specific regions (or modified versions thereof) of PXA1 (constructs 1 to 8, numbered on the left). n.s., results of the NRA were similar to those of yeast two-hybrid, but data are "not shown."
(C) Yeast two-hybrid assay showing the relative growth of yeast strains on media for either plasmid selection only (left panel) or high stringency conditions that are dependent on two-hybrid protein interactions (right panel). Numbers on the left correspond to PXA1-based constructs described in **(B)**. The dilution series was prepared by first adjusting the yeast cell culture density to 0.5 OD_{600}, then plating, from left to right, 5 μL of a 1:5 dilution series on the plates, with the 0.5 OD_{600} culture being the left-most spot.
(D) Coimmunoprecipitation of CGI-58 and PXA1. Whole-cell lysates from *Escherichia coli* expressing S-tagged CGI-58 or an empty vector were incubated with in vitro–synthesized full-length HA-tagged PXA1 and complexes were immunoprecipitated using anti-S-tag antibodies. PXA1-HA was detected by immunoblotting using anti-HA antibodies. The position of a molecular mass marker (117 kD) is shown to the left. A Coomassie blue–stained gel of lysates used to program the reactions, including an immunoblot of S-tagged CGI-58, is shown in Supplemental Figure 3 online.
(E) Nuclear relocalization results, whereby each row of epifluorescence micrographs shows a representative plant cell that is transiently coexpressing NLS-RFP alone (top row) or NLS-RFP fused to a portion of PXA1 (numbers correspond to PXA1-based constructs described in **[B]**) and GFP-CGI-58. Protein–protein interactions were scored based on recruitment of a portion of GFP-CGI-58 to the nucleus (white arrowheads). Bar = 10 μm.

or IAA in growth media represses root elongation of wild-type *Arabidopsis* plants, but *pxa1* mutant plants are resistant to the effects of IBA due to reduced transport into peroxisomes for conversion to IAA (Figures 5A and 5B) (Zolman et al., 2001). *cgi-58* mutant plants also displayed tolerance to IBA but showed an intermediate phenotype between wild-type and *pxa1* mutant seedlings (Figure 5B). Moreover, *cgi-58 pxa1* double mutant plants displayed a phenotype similar to the *pxa1* mutant alone, revealing an epistatic relationship of *PXA1* to *CGI-58* in the auxin signaling pathway. Similar inhibitory results were observed if the

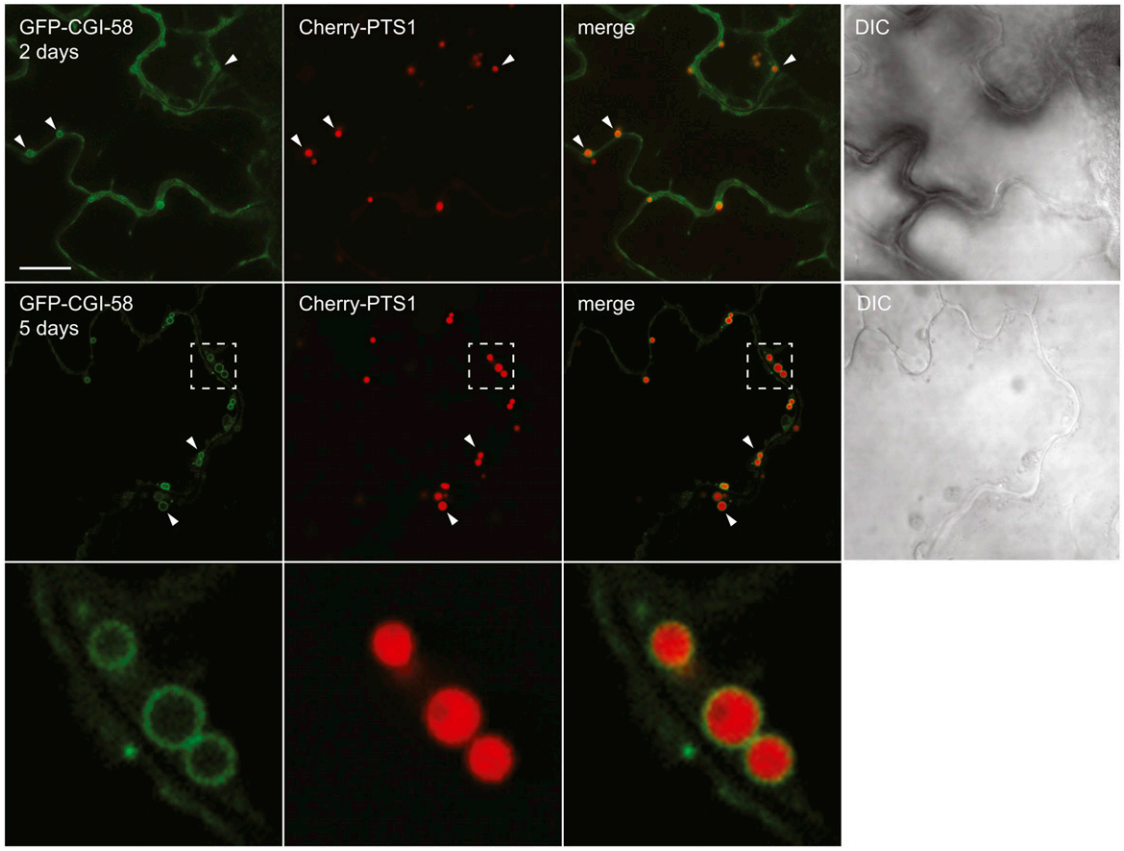

Figure 3. Localization of CGI-58 to the Cytosol and Peroxisomes in Tobacco Leaf Cells.

Shown are representative confocal micrographs of tobacco epidermal cells transiently cotransformed with GFP-CGI-58 and the peroxisomal matrix marker protein Cherry-PTS1 (consisting of the Cherry fluorescent protein linked to a type 1 peroxisomal targeting signal) at either 2 or 5 d after *Agrobacterium* coinfiltration. Arrowheads illustrate the localization of GFP-CGI-58 to the periphery of Cherry-PTS1–labeled peroxisomes. The bottom row of images shows a portion of the cell (dashed boxes in middle row) 5 d after *Agrobacterium* coinfiltration, shown at higher magnification. Shown also in the top two rows of images are the differential interference contrast (DIC) images of each cell to help delineate cell borders. Note that the majority of cell volume is occupied by the vacuole(s), and as such, the cytoplasm is mostly appressed into to a narrow region near the cell surface. Bar = 15 μm.

synthetic auxins 2,4-dichlorophenoxybutyric acid or 2,4-D, which are similar to IBA and IAA in that their conversion requires PXA1 (Hayashi et al., 2002), were used in the root bioassays (see Supplemental Figure 5A online) or if auxin sensitivity was measured using hypocotyl elongation assays (see Supplemental Figure 5B online). Collectively, these results demonstrate that auxin signaling pathways were similarly disrupted in at least two different organ types, both of which require PXA1 transport activity for full biological activity.

CGI-58 and PXA1 Cooperatively Regulate TAG Content in Leaves but Not in Seeds

Previous studies revealed that disruption of *CGI-58* or *PXA1* resulted in a significant increase in TAG content in plant leaves, particularly for TAG molecular species containing polyunsaturated FAs (Kunz et al., 2009; Slocombe et al., 2009; James et al., 2010). To directly compare changes in lipid content and composition, we analyzed LD abundance and individual TAG molecular species in leaves of wild-type, *pxa1*, *cgi-58*, and *cgi-58 pxa1* double mutant plants. As shown in Figure 6, disruption of either *cgi-58* or *pxa1* resulted in an increase in LD abundance in leaf mesophyll cells in comparison to the wild type. The abundance of LDs also was increased in the *cgi-58 pxa1* double mutant plants, but the increase was no greater than that of either single mutant alone (Figure 6A). Lipidomics analysis of leaf lipids revealed that the TAG pools in each mutant plant line were enriched in TAG molecular species containing polyunsaturated FAs, including 54:9 and 54:8 (Figure 6B). These data indicate that CGI-58 and PXA1 likely operate on the same or similar biochemical pathway(s) to limit TAG accumulation in plant leaves, particularly in regards to accumulation of TAGs containing polyunsaturated FAs, and that loss of PXA1 and/or CGI-58 activity results in enhanced TAG formation, perhaps due to reduced FA turnover.

Since PXA1 is known to play an essential role in turnover of FAs derived from TAGs in germinated seeds (Zolman et al., 2001; Footitt et al., 2002; Eastmond, 2006), we investigated whether CGI-58 also was required for the breakdown of FAs in support

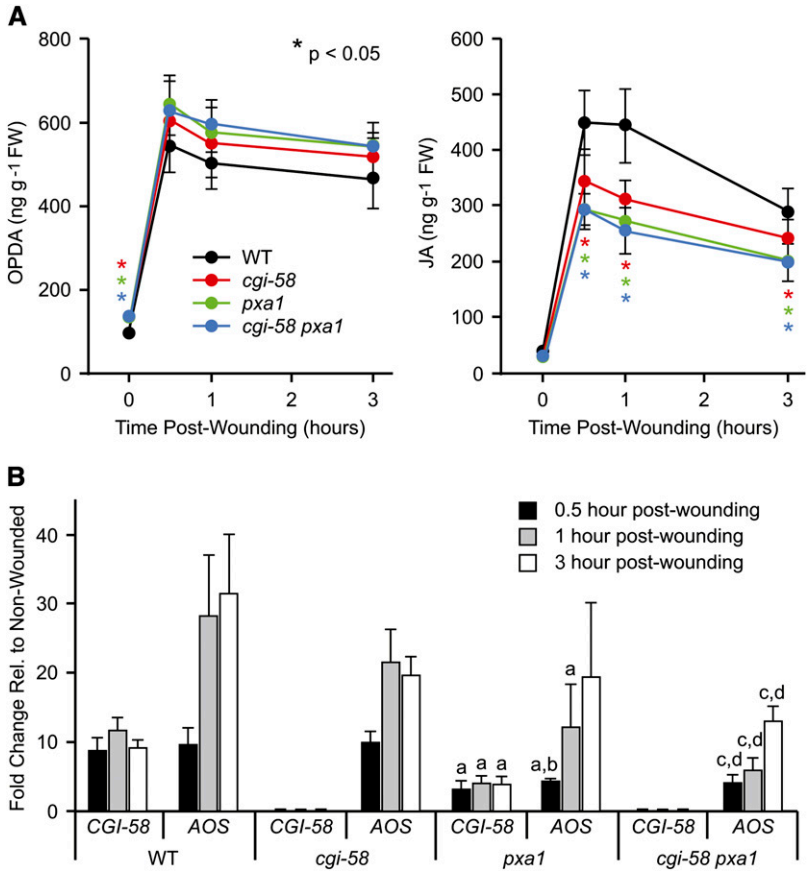

Figure 4. Evaluation of the JA Signaling Pathway in Wild-Type and *cgi-58*, *pxa1*, and *cgi-58 pxa1* Mutant *Arabidopsis* Plants in Response to Wounding.

(A) Plants were mechanically wounded and then amounts of OPDA (left graph) and JA (right graph) were measured over time. FW, fresh weight; WT, the wild type.

(B) Changes in *CGI-58* and *AOS* expression as measured by qRT-PCR. The plant genotype is shown at the bottom, and specific transcripts quantified are shown above. a = P < 0.05 between the wild type and *pxa1*; b = P < 0.05 between *cgi-58* and *pxa1*; c = P < 0.05 between the wild type and *cgi-58 pxa1*; d = P < 0.05 between *cgi-58* and *cgi-58 pxa1*.

Values in **(A)** and **(B)** represent averages and SD (n = 4).

of postgerminative growth. As shown in Figure 7A, *pxa1* mutant seedlings were unable to establish unless Suc was provided in the growth medium. However, the *cgi-58* mutant plants could establish in the absence of Suc, similar to the wild type, suggesting that TAG and FA breakdown was not compromised in the mutant plants. Measurement of FA content throughout seed germination and establishment confirmed that FAs were indeed broken down at similar rates in both wild-type and *cgi-58* mutant plants (Figure 7B). Taken together with the results described above, it is apparent that CGI-58 and PXA1 participate in regulating TAG content in non-lipid-storing mesophyll cells of plant leaves, but these functions apparently do not overlap in lipid storing cells of seeds.

DISCUSSION

CGI-58 plays a key role in regulating TAG metabolism and lipid signaling in mammals, and while some aspects of its biochemical activity are known, significant questions remain regarding its ability to participate in different cellular processes. In plants, CGI-58 was previously shown to be involved in regulating TAG metabolism in non-lipid-storing cell types (James et al., 2010), somewhat similar to what is observed in mammals, and, here, we further demonstrate that CGI-58 is involved in regulating at least two major lipid hormone-based pathways, including oxylipin production and auxin signaling. There are a number of possible mechanisms by which CGI-58 might contribute to regulating these various processes in plants and animals, including inherent enzyme activity, interaction with various protein partners, and production and/or regulation of lipid signals.

Potential Role(s) of CGI-58 Enzyme Activity in the Regulation of Lipid Metabolism and Signaling

As a member of the α/β hydrolase class of proteins, CGI-58 contains two domains that have potential for enzymatic involvement in lipid metabolism. One is a lipase/esterase-like domain that includes a G-x-S-x-G motif, where the Ser residue is essential for enzyme catalysis. In mammalian CGI-58, the Ser residue is substituted with

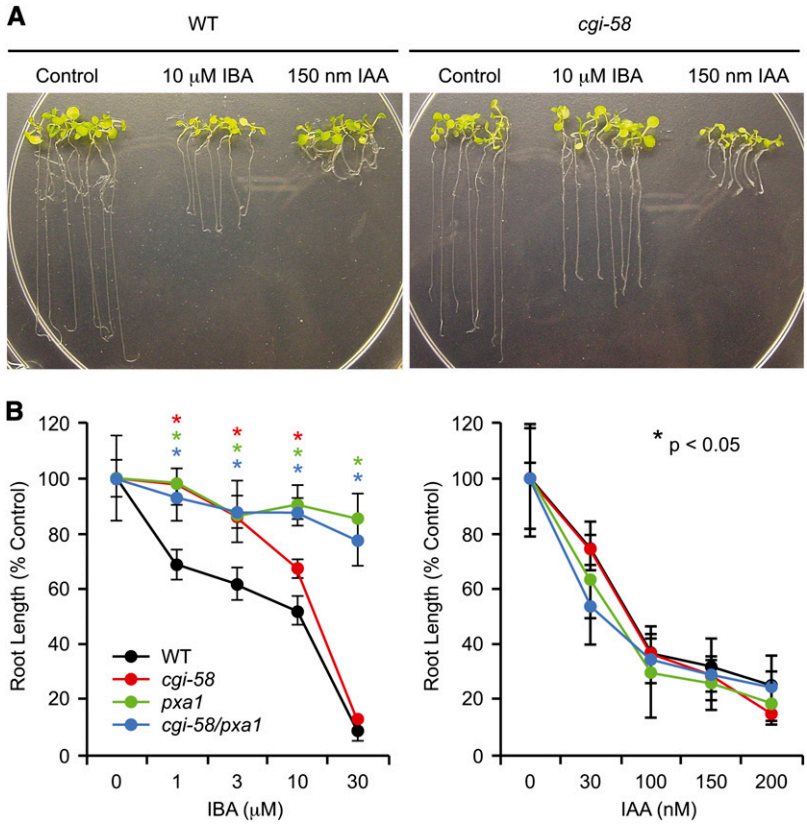

Figure 5. Measurement of Auxin Responses in Wild-Type and *cgi-58*, *pxa1*, and *cgi-58 pxa1* Mutant *Arabidopsis* Plants.

Seeds were germinated in media lacking hormones, transferred to plates lacking or containing the indicated amounts of IBA or IAA, and then grown under constant light for 8 d before root length was measured.

(A) Representative images of wild-type (WT) and *cgi-58* plants showing long root growth for each plant type on media lacking auxins (Control) but significantly shorter growth of wild-type plants when grown in the presence of IBA or IAA. Note that *cgi*-58 plants are resistant to the effects of IBA in comparison to the wild type.

(B) Dose–response curves showing resistance of various plant lines to IBA (left graph) and similar sensitivities to IAA (right graph). Values represent averages and SD ($n > 15$), and significant differences (indicated by asterisks; $P < 0.05$) are relative to the wild type.

Asn, and biochemical analysis suggests that the enzyme lacks any lipase activity (Lass et al., 2006; Yamaguchi et al., 2007; Ghosh et al., 2008). However, disruption of CGI-58 in mammals results in reduced lipase activity, and studies have shown that rather than catalyze TAG lipase activity directly, CGI-58 in mammals instead interacts with and stimulates the activity of a TAG lipase enzyme (Subramanian et al., 2004; Lass et al., 2006). For plant CGI-58, the Ser residue of the G-x-S-x-G motif is preserved (see Supplemental Figure 1 online), and biochemical studies revealed that the protein does indeed have lipase activity, although it is orders of magnitude lower than a typical lipase enzyme in plants (Ghosh et al., 2009). As such, it is possible that the disruption of *cgi-58* in plants results in elevated TAG content in leaves (Figure 6; James et al., 2010) due to a loss of lipase activity. However, several observations suggest that this is not the case. For instance, measurement of free FA content in *cgi-58* leaves showed that free FAs were elevated in comparison to the wild type (see Supplemental Figure 6 online), which would not be expected if CGI-58 was a lipase. In addition, the composition of the free FA pool was altered in favor of higher amounts of polyunsaturated FAs, and lipidomics analysis revealed that most of the major leaf glycerolipids, including galactolipids and phospholipids, showed a general increase in molecular species containing polyunsaturated FAs (see Supplemental Figure 6 online). As such, it appears that loss of *cgi-58* results in a general defect in turnover of major leaf FAs and that the reduction in FA breakdown would presumably lead to enhanced availability of these FAs for incorporation into various lipid classes. The observed increase in TAG content might serve as a buffer for overflow of excess acyl groups (Kunz et al., 2009; Hernández et al., 2012; Chapman et al., 2013).

The α/β hydrolase–type proteins also contain an acyltransferase domain, which includes an HxxxxD motif. This sequence is present in CGI-58 from both plant and animals, and expression of both proteins in yeast cells was associated with increased production of PA, suggesting that the enzymes have LPAAT activity (Ghosh et al., 2008, 2009; see Supplemental Figure 1 online). Indeed, characterization of enzyme activity in vitro showed a capacity for the enzymes to use acyl-CoA and lysophosphatidic acid as

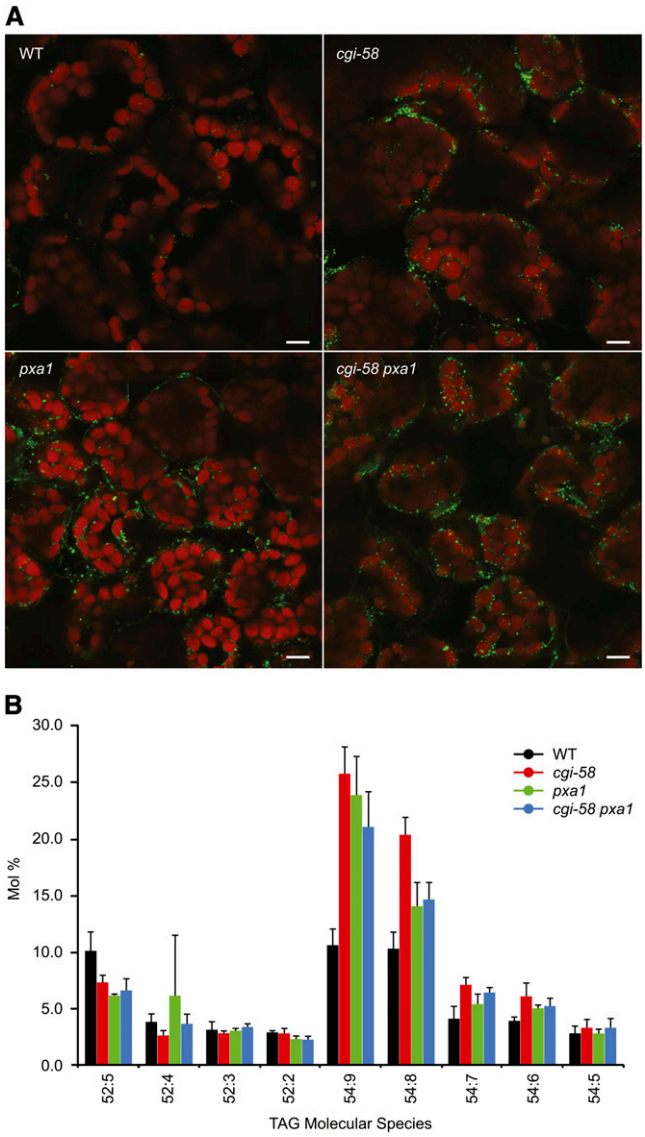

Figure 6. Analysis of LDs and TAG Composition in Leaves of Wild-Type and Mutant *Arabidopsis* Plants.

(A) Representative confocal fluorescence micrographs of mesophyll cells of mature (i.e., 35 d old) leaves from wild-type (WT) and *cgi-58*, *pxa1* and *cgi-58 pxa1* mutant plants. Chloroplast autofluorescence is red and LDs (stained with BODIPY 493/503) are green. Quantification revealed that the average numbers of LDs were approximately six- to sevenfold higher in all mutant cells compared with the wild-type, but the values were not statistically different between mutants. Bars = 10 μm.

(B) Compositional analysis of TAGs extracted from leaves of wild-type and *cgi-58*, *pxa1*, and *cgi-58 pxa1* mutant 35-d-old plants. Values represent averages and SD of five biological replicates.

substrates to produce PA (Ghosh et al., 2008, 2009; Montero-Moran et al., 2010). However, the contributions of LPAAT activity to changes in lipid metabolism and signaling in vivo are presently unclear. For instance, while disruption of CGI-58 activity in mice results in reduced PA production during tumor necrosis factor signaling (Lord et al., 2012), other studies have shown that total LPAAT activity was unaffected in skin tissues of CGI-58 disrupted mice (Radner et al., 2010). Furthermore, although LPAAT activity can contribute to the production of TAG by conversion of PA to the TAG precursor diacylglycerol, the LPAAT activity of CGI-58 is not likely to contribute significantly in this regard since TAGs are increased, and not decreased, in CGI-58 disrupted plants or animals. Furthermore, lipidomics analysis of plant leaves showed that PA content is increased in *cgi-58* leaves, and not decreased, in comparison to the wild type (see Supplemental Figure 6 online). As such, the specific role of LPAAT activity in lipid metabolism and signaling in both plants and animals remains to be clarified.

Potential Role(s) of CGI-58 Protein–Protein Interactions in Regulation of Lipid Metabolism and Signaling

Given the importance of protein–protein interactions in the activity of CGI-58 in stimulating TAG turnover in mammals (Subramanian et al., 2004; Yamaguchi et al., 2004; Lass et al., 2006), we used a two-hybrid screen to identify potential interacting protein partners that might be important for CGI-58 activity in plants. One of the proteins identified in this screen was the peroxisomal transport protein PXA1 (see Supplemental Table 1 online). Notably, only the C-terminal portion of PXA1, which is known to be oriented on the cytosolic side of peroxisomal membranes and is important for regulation of protein activity in vivo, was recovered in this assay. Additional support for a physical interaction between CGI-58 and PXA1 included coimmunoprecipitation of full-length proteins in vitro (Figure 2D) and mutagenesis studies of the C-terminal domain of PXA1, which showed a correlation between mutations to this region known to disrupt PXA1 activity in plants and loss of an ability to interact with CGI-58 (Figure 2B). Further evidence for a functional role of PXA1 in CGI-58 activity was the localization of CGI-58 to the surface of peroxisomes in vivo (Figure 3).

Given the known role of PXA1 in transporting FAs into peroxisomes for their subsequent breakdown, and the shared phenotype of an increase in TAG content in leaves disrupted in either CGI-58 or PXA1 activity (Figure 6; Kunz et al., 2009; Slocombe et al., 2009; James et al., 2010), our working hypothesis is that CGI-58 interacts with and somehow stimulates the transport activity of PXA1. Consistent with this hypothesis, loss of CGI-58 activity in plants showed reductions in jasmonate and auxin signaling (Figures 4 and 5; see Supplemental Figure 5 online) that were consistent with reduced activity of PXA1. It is conceivable that loss of *cgi-58* somehow indirectly affects PXA1 activity, perhaps through changes in membrane lipid composition that negatively impact transport activity. This seems highly unlikely, however, since *cgi-58* mutant plants show normal growth and development (James et al., 2010), and it is difficult to rationalize how loss of CGI-58 could specifically compromise PXA1 activity and not the hundreds of other membrane proteins in various organelles that are known to be essential for plant growth and development. Thus, the simplest explanation is that CGI-58 somehow regulates PXA1 activity. Since the levels of free FAs in *cgi-58* plants are somewhat elevated in comparison to the wild type, and this phenotype is exacerbated when the

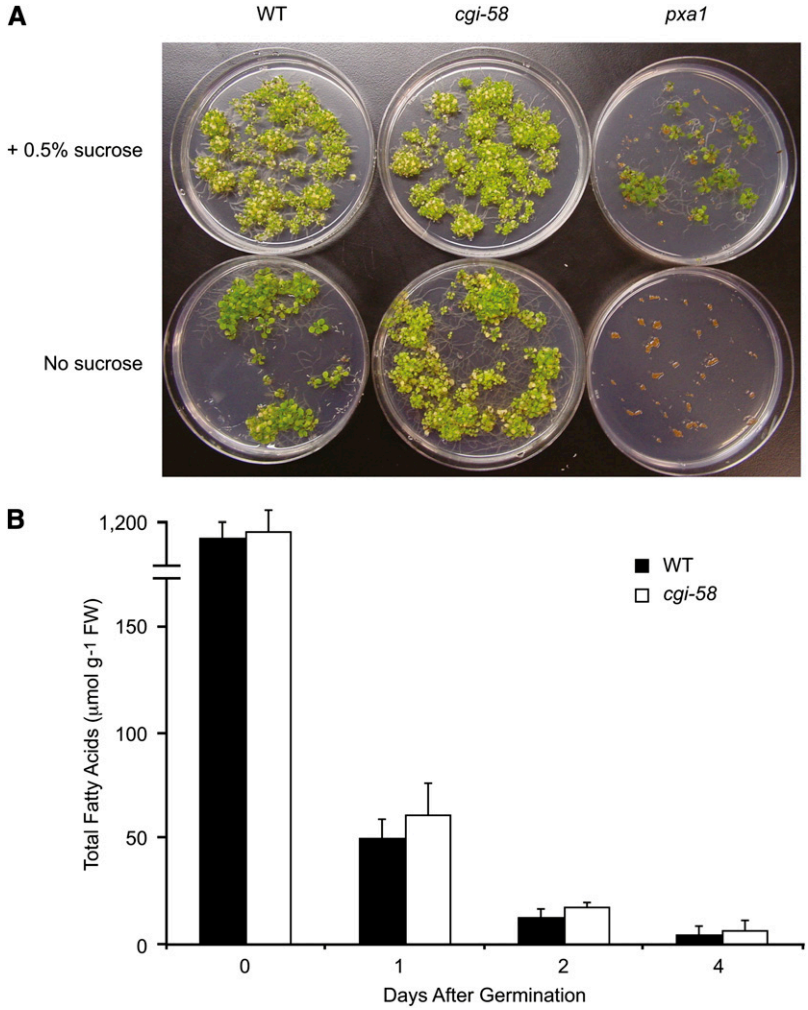

Figure 7. Measurement of Seedling Establishment and Seed Oil Breakdown in Wild-Type and Mutant *Arabidopsis* Plants.

(A) Seeds of the indicated plant lines were germinated on plant nutrient medium lacking or containing 0.5% Suc and then grown under constant light for 7 d. Note the inability of *pxa1* to grow in the absence of Suc, while *cgi-58* mutants are similar to the wild type (WT).
(B) Measurement of total FA content in germinating seedlings, illustrating that *CGI-58* is not required for the breakdown of FAs derived from storage oil. Values represent averages and SD (n = 4). FW, fresh weight.

cgi-58 plants are subject to wounding (see Supplemental Figure 6 online), one possibility is that CGI-58 serves as a scavenger for excess acyl-groups, either free FAs or acyl-CoAs, and delivers these to peroxisomes via transient interaction with PXA1 for their subsequent breakdown. Observations in support of this premise are that CGI-58 does indeed contain lipid binding domains (Ghosh et al., 2009), and perhaps these domains are used for lipid trafficking, rather than for enzymatic activity. However, prior experiments have demonstrated that exposure of *pxa1* plants to extended dark treatment resulted in plant death due to hyper-accumulation of free FAs (Kunz et al., 2009; Slocombe et al., 2009), and we did not observe this phenotype for dark-treated *cgi-58* mutant plants. These data suggest that CGI-58 is not absolutely required for the breakdown of free FAs, but rather contributes to PXA1-mediated transport and subsequent FA degradation. It is perhaps more difficult to envision how CGI-58 might also be involved in delivery of other lipid metabolites, such as OPDA and IBA, into peroxisomes via PXA1. However, it has already been noted that there are some structural similarities between FAs and these lipophilic hormones, and it is possible that a single protein might be capable of binding each metabolite (Theodoulou et al., 2005) (see Supplemental Figure 7 online). As a precedent, PXA1 is involved in transport of each of these substrates (Theodoulou et al., 2005).

A second, and perhaps more tantalizing, role for CGI-58 in stimulating PXA1 activity comes from a recent article demonstrating that PXA1 has inherent hydrolase activity toward acyl-CoA lipid substrates (De Marcos Lousa et al., 2013). For many years, it has been unclear whether PXA1 transports the free acid or CoA forms of lipid substrates, and there is evidence in support of both models (Footitt et al., 2002; Fulda et al., 2004; Linka et al., 2008; Nyathi et al., 2010). The article by De Marcos Lousa

et al. (2013) helps to reconcile these data, since the new model suggests that an acyl-CoA substrate is hydrolyzed by PXA1 as part of the transport process, which is followed by the subsequent resynthesis of an acyl-CoA in the matrix that is required for entry into the β-oxidation cycle. The observation that PXA1 is also a hydrolase enzyme suggests that CGI-58 might stimulate PXA1 in a manner that is somewhat similar to how CGI-58 stimulates the hydrolase activity of ATGL in mammalian cells. That is, in mammalian cells, CGI-58 promotes lipid turnover by stimulating the hydrolase activity of a lipase enzyme (Subramanian et al., 2004; Lass et al., 2006), while in plant cells, CGI-58 might promote lipid turnover by stimulating the hydrolase activity of PXA1. Notably, the details of this activation mechanism are not understood in either plants or animals, but the availability of an in vitro transport system for PXA1 provides an opportunity to explore these functional relationships further (De Marcos Lousa et al., 2013).

The interaction of CGI-58 with PXA1 in plants raises the intriguing question of whether mammalian CGI-58, or perhaps one or more of the other 18 α/β hydrolase-like proteins in humans (Li et al., 2009; Lord et al., 2013), might similarly interact with peroxisomal, or perhaps mitochondrial, ABC-type transport proteins to help facilitate the breakdown and/or further metabolism of various lipid substrates. Although human CGI-58 has not been shown to physically associate with any of the peroxisomal ABC transporters, a large-scale affinity-capture study that employed the peroxisomal ABC half-transporter PMP70 as bait revealed an association with another α/β hydrolase–type protein named the mesoderm-specific transcript protein (Ewing et al., 2007). The mesoderm-specific transcript protein, similar to CGI-58 in mammals, plays a key role in adipose tissue expansion and regulation and is itself regulated extensively by gene expression, alternative splicing, and epigenetics (Nikonova et al., 2008). An α/β hydrolase in yeast cells also has been identified whose disruption significantly altered the FA composition of cardiolipin in mitochondrial membranes (Beranek et al., 2009), demonstrating that α/β hydrolases can influence glycerolipid metabolism within this organelle. Taken together, it is possible that CGI-58–like proteins may regulate glycerolipid metabolism and energy maintenance in eukaryotic cells by interacting with proteins in multiple subcellular compartments.

However, it is also noteworthy that CGI-58 in mammals is known to have ATGL-independent functions, and it is presently unclear whether these functions include other interacting protein partners or inherent CGI-58 enzyme activity (Radner et al., 2011). This raises the possibility that CGI-58 in plants might also have PXA1-independent activities. Evidence in support of this premise comes from previous detailed lipidomic analyses of *cgi-58* and *pxa1* plants (Kunz et al., 2009; James et al., 2010), which revealed both similarities and differences in the lipid phenotypes. For instance, while TAG content was similarly increased in the mutant plants, *cgi-58* mutants also showed an increase in total galactolipid content, while the amount in *pxa1* remained unchanged. However, it is possible that these differences reflect differences in the experimental conditions or treatments employed. Still, it is likely that each of these proteins has functions that are independent of one another. Indeed, as described below, the activities of PXA1 and CGI-58 do not appear to overlap in germinating seeds.

Implications for Understanding CGI-58 Activity in Mammals and Production of Biofuels in Plants

That CGI-58 participates in the regulation of the jasmonate biosynthetic pathway in plants also raises the question of whether CGI-58 might play a similar role in regulating eicosanoid production in mammals. The jasmonate and eicosanoid pathways are similar in that they involve an initial release of polyunsaturated FAs from a glycerolipid precursor, followed by oxidative reactions that produce a variety of downstream signaling molecules, the end result of which is the activation of global effectors such as PPARs in mammals and COI1 in plants (Gfeller et al., 2010; Ballaré, 2011; Bozza et al., 2011). Notably, leukocytes in patients with Chanarin-Dorfman syndrome display a constitutive elevation of LDs (Lefèvre et al., 2001), a condition normally associated with induced eicosanoid synthesis (Bozza et al., 2011), and knockdown of *CGI-58* results in downregulation of PPARα-sensitive gene expression in mice (Brown et al., 2010). As such, it is not unreasonable to speculate that CGI-58–mediated lipolysis and/or acyltransferase activity generates a lipid signal(s) essential to this process in mammals.

Finally, it is apparent from our studies, as well as those conducted in mammals, that CGI-58 activity can vary depending on tissue and/or organ type. For instance, although the working model for CGI-58 regulation of TAG breakdown in mammals involves protein interaction–dependent stimulation of ATGL activity in lipid-storing adipocytes, disruption of *CGI-58* results in hyperaccumulation of lipids in non-lipid-storing cell types, such as cells of skin, liver, and muscle (Radner et al., 2011). Likewise, in plants, it appears that CGI-58 functions primarily in the regulation of lipid metabolism and signaling in non-lipid-storing cell types, rather than in lipid storing tissues such as seeds (Figures 6 and 7; James et al., 2010; Kelly et al., 2011). On the other hand, CGI-58 in plants belongs to a large family of α/β hydrolase–like proteins (Ghosh et al., 2009), and perhaps another member of the family is involved in stimulating PXA1 activity in seeds. Regardless, the accumulation of lipids in *cgi-58* leaves, with no obvious effects on seed development, germination, or seedling establishment, provides an opportunity to consider practical applications of these results. There is increasing interest in developing metabolic engineering strategies to enhance the accumulation of energy-dense TAGs in leaf tissues, which could subsequently be extracted for use in biofuels (Chapman et al., 2013). Suppression of CGI-58 activity, rather than PXA1, would be advantageous for this process since loss of CGI-58 results in elevated TAG in leaves, similar to that of *pxa1* plants (Figure 6; Kunz et al., 2009; Slocombe et al., 2009; James et al., 2010), but *cgi-58* mutant plants do not show the pronounced negative effects on seed germination and seedling establishment, as observed for *pxa1* (Figure 7; Zolman et al., 2001; Footitt et al., 2002; Eastmond, 2006; Kanai et al., 2011). Thus, continued studies of CGI-58 and PXA1 will illuminate not only novel aspects of plant lipid metabolism and signaling, but also may provide opportunities for producing high amounts renewable fuels and chemicals in plants.

METHODS

Plant Material

Plant lines included wild-type *Arabidopsis thaliana* (Columbia-0 [Col-0]), the *cgi-58* mutant (SALK collection number 136871; Col-0 background; homozygous T-DNA disrupted line; James et al., 2010), and the *pxa1* mutant (an ethyl methanesulfonate–generated, splice-site mutant of Col-0; Zolman et al., 2001; kindly provided by Ian Graham, University of York). The *pxa1 cgi-58* double mutant was generated by crossing *pxa1* and *cgi-58* plants, and progeny harboring at least one disrupted allele of *cgi-58* were identified by PCR-based genotyping, as described (James et al., 2010). Plants homozygous for *pxa1* were subsequently identified in the next generation by an inability of seedlings to establish in media lacking Suc (Eastmond, 2006) and then plants were recovered and genotyped to identify those plants that were homozygous for *cgi-58*. All *Arabidopsis* plants were grown in chambers at 21°C with a 16-h/8-h light/dark cycle. Seeds were typically surface sterilized and sown in plant nutrient media (Haughn and Somerville, 1986) or half-strength Murashige and Skoog salts (Murashige and Skoog, 1962) containing 0.5% Suc and solidified with 0.6% (w/v) agar for various growth assays. Tobacco (*Nicotiana tabacum* cv Xanthi) plants were grown in chambers at 21°C with a 16-h/8-h light/dark cycle. Tobacco (*N. tabacum* cv Bright Yellow-2) suspension cell cultures were maintained as described (Dhanoa et al., 2010).

Lipid Extraction and Analysis

Total lipids were extracted from combined leaves of mature plants (35-d old, two plants per sample) and fractionated as described previously (Chapman and Moore, 1993; James et al., 2010). Lipid species were identified and quantified by direct-infusion, electrospray ionization–mass spectrometry (Bartz et al., 2007) using a Waters Micromass Quattro Ultima triple quadrupole MS (Waters). TAG molecular species were quantified in full scan mode with acyl species identified by neutral loss fragmentation spectra in tandem mass spectrometry scans with a collision energy of 30 V (Bartz et al., 2007). Tripentadecanoyl glycerol (tri-15:0) was added at the time of extraction and used as a quantitative standard for TAG content. Polar lipids, including phosphatidylcholine, monogalactosyldiacylglycerol, and digalactosyldiacylglycerol, were quantified based on a di-14:0 phosphatidylethanolamine internal standard. Typical scanning conditions for a direct infusion rate of 12.5 μL/min were performed in positive ion mode with a 3- to 3.5-kV spray voltage, 40-V cone voltage, and a scan mass-to-charge ratio range of 100 to 1050. The desolvation and source temperatures were maintained at 200 and 80°C, respectively, and the desolvation and cone gas flows were set at 200 and 80 L/h, respectively. Lipid standards were purchased from Avanti Polar Lipids. For free FA analysis, total lipid extracts were derivatized with 1-ethyl-3-(3-dimethylaminopropylcarbodiimide) and then quantified by gas chromatography–mass spectrometry relative to a 17:0 spiked internal standard. Fourteen-day-old wild-type and *cgi-58* mutant seedlings were grown in liquid half-strength Murashige and Skoog media, wounded with forceps, and then five biological replicates were collected and extracted for total lipids at t = 0 and 3 h postwounding.

Plasmid Construction

For yeast two-hybrid analysis, the full-length *Arabidopsis* CGI-58L and CGI-58S open reading frames (ORFs) (James et al., 2010) (see Supplemental Figure 1 online) were amplified by PCR using appropriate primers (sequences of all primers used in this study are available upon request), and then PCR products were purified, digested with *Eco*RI and *Bam*HI, and subcloned into similarly digested bait vector pGBKT7-DNA-BD (Clontech). Modifications to sequences encoding the C terminus of NBD2-B in PXA1, including replacement of the last 31 codons with 19 codons that correspond to the *pxa1* mutant (Zolman et al., 2001) (see Supplemental Figure 2 online) or a point mutation changing Asp at position 1276 to Asn (Dietrich et al., 2009) (see Supplemental Figure 2 online), were introduced by PCR-based mutagenesis. The PXA1-NBD1-A and/or B regions (corresponding to the same regions present in the NBD2 sequence; see Supplemental Figure 2 online) were cloned into yeast two-hybrid pGADT7-AD (Clontech) and nuclear relocalization (pRLT2/NLS-RFP; Dhanoa et al., 2010) assay vectors by PCR amplification of the appropriate region of the PXA1 cDNA (Zolman et al., 2001) (kindly provided by Bonnie Bartel, Rice University). Construction of the nuclear relocalization assay vector pRTL2/GFP-CGI-58, encoding a GFP-tagged version of CGI-58L, was described (James et al., 2010). Subcloning of the CGI-58L ORF into the pMDC43 binary vector was performed using Gateway technology (Curtis and Grossniklaus, 2003), which resulted in an in-frame fusion between GFP and CGI-58. Binary vectors expressing either Cherry-PTS1 alone or GFP and Cherry-PTS1 were constructed using the pSAT and pRCS2 vectors (Chung et al., 2005), as described (Ching et al., 2012). For coimmunoprecipitation experiments, the full-length PXA1 and CGI-58L ORFs were amplified by PCR using appropriate primers, then PCR products were purified, digested with *Eco*RI and *Bam*HI or *Bam*HI and *Hin*dIII, and subcloned into similarly digested pGADT7 and pET29a+ (Novagen), yielding pGADT7/PXA1 and pET29a+/CGI-58, respectively.

Yeast Two-Hybrid Analysis

An *Arabidopsis* cDNA expression library (normalized from various plant tissues and cloned into the appropriate prey vector; Clontech) was screened with the Matchmaker Gold Yeast Two-Hybrid System (Clontech) using *Arabidopsis* CGI-58 as bait. Briefly, the bait plasmid was transformed into the haploid yeast strain Y2H Gold, and then transgenic yeast cells were mated with complementary yeast cells harboring the *Arabidopsis* expression library. Initial selection of interacting proteins was conducted by plating mated cells on media lacking Trp and Leu (which ensures the diploid yeast cells contain both the bait and prey plasmids) and containing X-α-Gal (which is converted into a blue-colored product if the *MEL1* reporter gene is activated) and Aureobasidin A (which normally kills yeast cells but is detoxified by expression and activity of the *AUR1-C* reporter gene). Colonies were subsequently patched onto higher stringency plates prepared as above but additionally lacking in His and adenine, which are synthesized by the enzymes encoded by the *HIS* and *ADE* reporter genes. Yeast strains that grew on the former, lower selection plates were designated "weak" interactors, while strains growing on both low and high stringency conditions were designated as "strong" interactors. Plasmids were extracted from yeast cells to determine the identity of encoded prey proteins by DNA sequencing, and plasmids were retransformed into yeast cells with appropriate empty vector controls to test for autoactivation.

Coimmunoprecipitation Assays

Full-length HA-tagged PXA1 was synthesized in vitro using the TNT T7 Coupled Reticulocyte Lysate System (Promega) according to the manufacturer's protocol, with pGADT7/PXA1 serving as template plasmid DNA. Equal amounts of total *Escherichia coli* protein lysates containing recombinant S-tagged CGI-58 or no recombinant protein (i.e., *E. coli* transformed with empty pET29a+ vector) were immobilized onto S-protein agarose (Novagen) and incubated with an aliquot of in vitro–synthesized HA-PXA1 for 2 h at 4°C. Beads were then collected by centrifugation and washed three times, then boiled in SDS-PAGE loading buffer and proteins separated by SDS-PAGE, blotted on nitrocellulose, and probed with either anti-HA antibodies (Bethyl Laboratories) to detect HA-PXA1 (Figure 2D) or anti-S-tag antibodies (Novagen) to detect S-tagged CGI-58 (see Supplemental Figure 3 online).

Nuclear Relocalization Assays

Nuclear relocalization assays were performed as described (Dhanoa et al., 2010). Transient cotransformations of Bright Yellow-2 cells were performed using 10 and 1 μg of the plasmids encoding GFP-CGI-58 and the various NLS-RFP fusion proteins, respectively, and a biolistic particle delivery system (Bio-Rad Laboratories), as described (Dhanoa et al., 2010). Following bombardment, cells were incubated for ~6 h to allow for gene expression and the intracellular sorting of the introduced gene products and then fixed in formaldehyde and viewed using a Zeiss Axioscope 2 MOT epifluorescence microscope (Carl Zeiss). Image capture was performed using a Retiga 1300 charge-coupled device camera (Qimaging) and Openlab 5.0 software (Improvision). All fluorescence images of cells shown in the figures are representative of >50 independent (transient) transformations from at least two independent cotransformation experiments.

Agrobacterium tumefaciens–Mediated Transient Transformation of Tobacco Leaves

Leaves of 4-week-old tobacco plants were infiltrated or coinfiltrated with *Agrobacterium* (strain LBA4404) carrying the appropriate binary vectors. Procedures for *Agrobacterium* growth, transformation, infiltration, and processing of leaf material for microscopy are described (McCartney et al., 2005). Confocal laser scanning microscopy images of (co)transformed epidermal and/or mesophyll cells were acquired 2 to 5 d after infiltration using a Leica DM RBE microscope. Fluorophore emissions were collected sequentially; single-labeling experiments showed no detectable crossover at the settings used for data collection. Confocal images were acquired as a Z-series of representative cells, and single optical sections were saved as 512 × 512-pixel digital images. All fluorescence images of *Agrobacterium*-transformed epidermal cells shown in Figure 3 and Supplemental Figure 4 online are representative of >30 cells from at least two independent (co)transformation experiments.

Imaging LDs in Situ

LDs in the mesophyll cells of leaves from ~3-week-old wild-type and mutant *Arabidopsis* plants were imaged after BODIPY 493/503 staining (Life Technologies) by confocal laser scanning fluorescence microscopy using BODIPY493 as described (James et al., 2010), except that images were acquired with a Zeiss LSM700 microscope (Carl Zeiss Microscopy). LD numbers were quantified using the Zeiss Zen Blue (2011 edition) software.

Plant Wounding and JA Analysis

Eight-day-old *Arabidopsis* seedlings grown in half-strength Murashige and Skoog liquid media were wounded with forceps. JA and OPDA were extracted from seedlings in 30 mM imidazole buffer, pH 7.0, in 70% isopropanol at 0.5, 1, and 3 h after wounding. Unwounded seedlings were maintained for all treatments as a control. One-hundred nanograms of D5-JA (C/D/N Isotopes) was added to all samples as an internal standard. Samples were incubated overnight at 4°C and then centrifuged at 10,000*g* for 10 min. The supernatant was then combined with three consecutive extractions in 2 mL of 100% isopropanol. JA and OPDA were further purified by solid phase extraction (NH2-SPE columns; Grace Davison Discovery Science) and reverse-phase HPLC (150 × 4.6-mm C18, Nucleosil 120-5; Macherey-Nagel). JA and OPDA were quantified against the D5-JA standard by gas chromatograph–mass spectrometry as methyl ester (derivatized in ethereal diazomethane) (Kilaru et al., 2007). JA and OPDA levels were quantified in triplicate at 0.5, 1, and 3 h after wounding as described above, and the experiments were repeated at least twice.

qRT-PCR

Ten-day-old wild-type, *cgi-58*, *pxa1*, and *cgi-58 pxa1* seedlings (grown in liquid medium) were mechanically wounded with a hemostat and, either 0.5, 1, or 3 h after wounding, tissues samples were flash frozen in liquid nitrogen. RNA was extracted using an RNeasy Plant Mini Kit (Qiagen). qRT-PCR was performed using the One-Step Ex Tag qRT-PCR kit (Takara Bio) with SYBR Green (Life Technologies) indicator dye. All amplifications started at 42°C for 15 min followed by a step at 95°C for 110 s. CGI-58L transcripts were amplified through 40 cycles of 94°C for 10 s, 62°C for 25 s, and 72°C for 20 s. AOS transcripts were amplified through 40 cycles of 94°C for 10 s, 57°C for 25 s, and 72°C for 20 s. Ef1α transcripts (used as an internal control) were amplified through 40 cycles of 94°C for 10 s, 56°C for 25 s, and 72°C for 20 s. All samples were subjected also to a melt curve between 65 and 95°C, increasing at 0.2°C/s. Primer efficiency (~100%) was assessed by subcloning each amplicon into the TOPO TA cloning vector (Life Technologies) followed by quantitative PCR on log dilutions of each plasmid. Fold changes were calculated for each transcript and a Student's *t* test was used to determine statistically significant differences between transcripts.

Hypocotyl and Root Elongation Assays

Seeds were surface sterilized, plated on medium containing 0.5% Suc (PNS medium) (Zolman et al., 2001; Strader et al., 2011), and then stratified for 3 d in the dark at 4°C. For root elongation assays, plates were subsequently incubated in constant light for 3 d, and then plants were transferred to fresh PNS plates lacking or containing the indicated amounts of hormones and incubated for 8 d in constant light. Plants were then removed and the primary root length measured. Representative plants from each treatment were grouped and aligned on new agar plates and photographed. For hypocotyl elongation assays, seeds were stratified as above, plates were incubated in the light for 24 h to induce seed germination, and then seeds were transferred to fresh PNS plates lacking or containing the indicated hormones and incubated in the dark for 4 d prior to measuring hypocotyl lengths. At least 15 independent seeds or plants were evaluated for each treatment, and experiments were repeated at least three times.

Accession Numbers

Sequence data from this article can be found in the Arabidopsis Genome Initiative under accession numbers At4g24160 (CGI-58) and At4g39850 (PXA1).

Supplemental Data

The following materials are available in the online version of this article.

Supplemental Figure 1. Comparison of the Polypeptide Sequences of *Arabidopsis* CGI-58 Long and Short Isoforms.

Supplemental Figure 2. Comparison of the Polypeptide Sequences of the N- and C-Terminal Halves of PXA1.

Supplemental Figure 3. Coimmunoprecipitation of CGI-58 and PXA1.

Supplemental Figure 4. Localization of GFP and GFP-CGI-58 in Tobacco Leaf Cells.

Supplemental Figure 5. Effects of Natural and Synthetic Auxins on Root and Hypocotyl Elongation in Wild-Type and Various Mutant *Arabidopsis* Plants.

Supplemental Figure 6. Lipidomics Analysis of Wild-Type and *cgi-58* Mutant *Arabidopsis* Plants.

Supplemental Figure 7. Comparison of the Molecular Structures for Linolenic Acid, OPDA, IBA, and 2,4-DB.

Supplemental Table 1. Identification and Characterization of Putative CGI-58-Interacting Proteins.

ACKNOWLEDGMENTS

We thank Bonnie Bartel (Rice University) for kindly providing the *PXA1* cDNA. This research was supported by funds from the U.S. Department of Energy, Office of Science (Biological and Environmental Research) (DE-SC0000797) to K.D.C., R.T.M., and J.M.D.; the University of Guelph Research Chairs Program and a grant from the Natural Sciences and Engineering Research Council of Canada (217291) to R.T.M.; the USDA (5347-21000-005-00D) to J.M.D.; and grants from the USDA (STELLAR 2007-38422-18084) and the National Science Foundation (DUE 0703118) to D.C.S. Confocal fluorescence imaging at the University of North Texas was made possible through a Major Research Instrumentation Grant from the National Science Foundation (1126205).

AUTHOR CONTRIBUTIONS

S.P., S.K.G., C.N.J., P.J.H., N.K., D.C.S., and J.K. performed experiments. All authors analyzed data, and K.D.C., R.T.M., and J.M.D. designed experiments and wrote the article.

Received March 25, 2013; revised April 17, 2013; accepted April 23, 2013; published May 10, 2013.

REFERENCES

Ballaré, C.L. (2011). Jasmonate-induced defenses: A tale of intelligence, collaborators and rascals. Trends Plant Sci. **16:** 249–257.

Bartz, R., Li, W.H., Venables, B., Zehmer, J.K., Roth, M.R., Welti, R., Anderson, R.G., Liu, P., and Chapman, K.D. (2007). Lipidomics reveals that adiposomes store ether lipids and mediate phospholipid traffic. J. Lipid Res. **48:** 837–847.

Beranek, A., Rechberger, G., Knauer, H., Wolinski, H., Kohlwein, S.D., and Leber, R. (2009). Identification of a cardiolipin-specific phospholipase encoded by the gene CLD1 (YGR110W) in yeast. J. Biol. Chem. **284:** 11572–11578.

Bozza, P.T., Bakker-Abreu, I., Navarro-Xavier, R.A., and Bandeira-Melo, C. (2011). Lipid body function in eicosanoid synthesis: An update. Prostaglandins Leukot. Essent. Fatty Acids **85:** 205–213.

Brown, J.M., et al. (2010). CGI-58 knockdown in mice causes hepatic steatosis but prevents diet-induced obesity and glucose intolerance. J. Lipid Res. **51:** 3306–3315.

Chapman, K.D., Dyer, J.M., and Mullen, R.T. (2012). Biogenesis and functions of lipid droplets in plants: Thematic Review Series: Lipid Droplet Synthesis and Metabolism: From Yeast to Man. J. Lipid Res. **53:** 215–226.

Chapman, K.D., Dyer, J.M., and Mullen, R.T. (2013). Commentary: Why don't plant leaves get fat? Plant Sci. **207:** 128–134.

Chapman, K.D., and Moore, T.S., Jr.,. (1993). N-acylphosphatidylethanolamine synthesis in plants: Occurrence, molecular composition, and phospholipid origin. Arch. Biochem. Biophys. **301:** 21–33.

Ching, S.L.K., Gidda, S.K., Rochon, A., van Cauwenberghe, O.R., Shelp, B.J., and Mullen, R.T. (2012). Glyoxylate reductase isoform 1 is localized in the cytosol and not peroxisomes in plant cells. J. Integr. Plant Biol. **54:** 152–168.

Chung, S.M., Frankman, E.L., and Tzfira, T. (2005). A versatile vector system for multiple gene expression in plants. Trends Plant Sci. **10:** 357–361.

Curtis, M.D., and Grossniklaus, U. (2003). A gateway cloning vector set for high-throughput functional analysis of genes *in planta*. Plant Physiol. **133:** 462–469.

Dave, A., Hernández, M.L., He, Z., Andriotis, V.M., Vaistij, F.E., Larson, T.R., and Graham, I.A. (2011). 12-Oxo-phytodienoic acid accumulation during seed development represses seed germination in *Arabidopsis*. Plant Cell **23:** 583–599.

De Marcos Lousa, C., Dietrich, D., Johnson, B., Baldwin, S.A., Holdsworth, M.J., Theodoulou, F.L., and Baker, A. (2009). The NBDs that wouldn't die: A cautionary tale of the use of isolated nucleotide binding domains of ABC transporters. Commun. Integr. Biol. **2:** 97–99.

De Marcos Lousa, C., van Roermund, C.W., Postis, V.L., Dietrich, D., Kerr, I.D., Wanders, R.J., Baldwin, S.A., Baker, A., and Theodoulou, F.L. (2013). Intrinsic acyl-CoA thioesterase activity of a peroxisomal ATP binding cassette transporter is required for transport and metabolism of fatty acids. Proc. Natl. Acad. Sci. USA **110:** 1279–1284.

Dhanoa, P.K., Richardson, L.G., Smith, M.D., Gidda, S.K., Henderson, M.P., Andrews, D.W., and Mullen, R.T. (2010). Distinct pathways mediate the sorting of tail-anchored proteins to the plastid outer envelope. PLoS ONE **5:** e10098.

Dietrich, D., Schmuths, H., De Marcos Lousa, C., Baldwin, J.M., Baldwin, S.A., Baker, A., Theodoulou, F.L., and Holdsworth, M.J. (2009). Mutations in the *Arabidopsis* peroxisomal ABC transporter COMATOSE allow differentiation between multiple functions *in planta*: Insights from an allelic series. Mol. Biol. Cell **20:** 530–543.

Eastmond, P.J. (2006). SUGAR-DEPENDENT1 encodes a patatin domain triacylglycerol lipase that initiates storage oil breakdown in germinating *Arabidopsis* seeds. Plant Cell **18:** 665–675.

Ewing, R.M., et al. (2007). Large-scale mapping of human protein-protein interactions by mass spectrometry. Mol. Syst. Biol. **3:** 89.

Footitt, S., Slocombe, S.P., Larner, V., Kurup, S., Wu, Y., Larson, T., Graham, I., Baker, A., and Holdsworth, M. (2002). Control of germination and lipid mobilization by COMATOSE, the *Arabidopsis* homologue of human ALDP. EMBO J. **21:** 2912–2922.

Fulda, M., Schnurr, J., Abbadi, A., Heinz, E., and Browse, J. (2004). Peroxisomal Acyl-CoA synthetase activity is essential for seedling development in *Arabidopsis thaliana*. Plant Cell **16:** 394–405.

Gfeller, A., Dubugnon, L., Liechti, R., and Farmer, E.E. (2010). Jasmonate biochemical pathway. Sci. Signal. **3:** cm3.

Ghosh, A.K., Chauhan, N., Rajakumari, S., Daum, G., and Rajasekharan, R. (2009). At4g24160, a soluble acyl-coenzyme A-dependent lysophosphatidic acid acyltransferase. Plant Physiol. **151:** 869–881.

Ghosh, A.K., Ramakrishnan, G., Chandramohan, C., and Rajasekharan, R. (2008). CGI-58, the causative gene for Chanarin-Dorfman syndrome, mediates acylation of lysophosphatidic acid. J. Biol. Chem. **283:** 24525–24533.

Haughn, G.W., and Somerville, C. (1986). Sulfonylurea-resistant mutants of *Arabidopsis thaliana*. Mol. Gen. Genet. **204:** 430–434.

Hayashi, M., Nito, K., Takei-Hoshi, R., Yagi, M., Kondo, M., Suenaga, A., Yamaya, T., and Nishimura, M. (2002). Ped3p is a peroxisomal ATP-binding cassette transporter that might supply substrates for fatty acid β-oxidation. Plant Cell Physiol. **43:** 1–11.

Hernández, M.L., Whitehead, L., He, Z., Gazda, V., Gilday, A., Kozhevnikova, E., Vaistij, F.E., Larson, T.R., and Graham, I.A. (2012). A cytosolic acyltransferase contributes to triacylglycerol synthesis in sucrose-rescued *Arabidopsis* seed oil catabolism mutants. Plant Physiol. **160:** 215–225.

Igal, R.A., and Coleman, R.A. (1996). Acylglycerol recycling from triacylglycerol to phospholipid, not lipase activity, is defective in neutral lipid storage disease fibroblasts. J. Biol. Chem. **271:** 16644–16651.

James, C.N., Horn, P.J., Case, C.R., Gidda, S.K., Zhang, D., Mullen, R.T., Dyer, J.M., Anderson, R.G., and Chapman, K.D. (2010). Disruption of the *Arabidopsis* CGI-58 homologue produces Chanarin-Dorfman-like lipid droplet accumulation in plants. Proc. Natl. Acad. Sci. USA **107:** 17833–17838.

Kanai, M., Nishimura, M., and Hayashi, M. (2010). A peroxisomal ABC transporter promotes seed germination by inducing pectin degradation under the control of ABI5. Plant J. **62:** 936–947.

Kelly, A.A., Quettier, A.L., Shaw, E., and Eastmond, P.J. (2011). Seed storage oil mobilization is important but not essential for germination or seedling establishment in *Arabidopsis*. Plant Physiol. **157:** 866–875.

Kilaru, A., Bailey, B.A., and Hasenstein, K.H. (2007). *Moniliophthora perniciosa* produces hormones and alters endogenous auxin and salicylic acid in infected cocoa leaves. FEMS Microbiol. Lett. **274:** 238–244.

Kunz, H.H., Scharnewski, M., Feussner, K., Feussner, I., Flügge, U.I., Fulda, M., and Gierth, M. (2009). The ABC transporter PXA1 and peroxisomal β-oxidation are vital for metabolism in mature leaves of *Arabidopsis* during extended darkness. Plant Cell **21:** 2733–2749.

Lass, A., Zimmermann, R., Haemmerle, G., Riederer, M., Schoiswohl, G., Schweiger, M., Kienesberger, P., Strauss, J.G., Gorkiewicz, G., and Zechner, R. (2006). Adipose triglyceride lipase-mediated lipolysis of cellular fat stores is activated by CGI-58 and defective in Chanarin-Dorfman Syndrome. Cell Metab. **3:** 309–319.

Lefèvre, C., et al. (2001). Mutations in CGI-58, the gene encoding a new protein of the esterase/lipase/thioesterase subfamily, in Chanarin-Dorfman syndrome. Am. J. Hum. Genet. **69:** 1002–1012.

Li, F., Fei, X., Xu, J., and Ji, C. (2009). An unannotated α/β hydrolase superfamily member, ABHD6 differentially expressed among cancer cell lines. Mol. Biol. Rep. **36:** 619–626.

Linka, N., Theodoulou, F.L., Haslam, R.P., Linka, M., Napier, J.A., Neuhaus, H.E., and Weber, A.P. (2008). Peroxisomal ATP import is essential for seedling development in *Arabidopsis thaliana*. Plant Cell **20:** 3241–3257.

Lord, C.C., et al. (2012). CGI-58/ABHD5-derived signaling lipids regulate systemic inflammation and insulin action. Diabetes **61:** 355–363.

Lord, C.C., Thomas, G., and Brown, J.M. (2013). Mammalian alpha beta hydrolase domain (ABHD) proteins: Lipid metabolizing enzymes at the interface of cell signaling and energy metabolism. Biochim. Biophys. Acta **1831:** 792–802.

McCartney, A.W., Greenwood, J.S., Fabian, M.R., White, K.A., and Mullen, R.T. (2005). Localization of the tomato bushy stunt virus replication protein p33 reveals a peroxisome-to-endoplasmic reticulum sorting pathway. Plant Cell **17:** 3513–3531.

Montero-Moran, G., Caviglia, J.M., McMahon, D., Rothenberg, A., Subramanian, V., Xu, Z., Lara-Gonzalez, S., Storch, J., Carman, G.M., and Brasaemle, D.L. (2010). CGI-58/ABHD5 is a coenzyme A-dependent lysophosphatidic acid acyltransferase. J. Lipid Res. **51:** 709–719.

Murashige, T., and Skoog, F. (1962). A revised medium for rapid growth and bioassays with tobacco tissue cultures. Physiol. Plant. **15:** 473–497.

Nikonova, L., Koza, R.A., Mendoza, T., Chao, P.M., Curley, J.P., and Kozak, L.P. (2008). Mesoderm-specific transcript is associated with fat mass expansion in response to a positive energy balance. FASEB J. **22:** 3925–3937.

Nyathi, Y., De Marcos Lousa, C., van Roermund, C.W., Wanders, R.J., Johnson, B., Baldwin, S.A., Theodoulou, F.L., and Baker, A. (2010). The *Arabidopsis* peroxisomal ABC transporter, comatose, complements the *Saccharomyces cerevisiae pxa1 pxa2*Δ mutant for metabolism of long-chain fatty acids and exhibits fatty acyl-CoA-stimulated ATPase activity. J. Biol. Chem. **285:** 29892–29902.

Radner, F.P., Grond, S., Haemmerle, G., Lass, A., and Zechner, R. (2011). Fat in the skin: Triacylglycerol metabolism in keratinocytes and its role in the development of neutral lipid storage disease. Dermatoendocrinol **3:** 77–83.

Radner, F.P., et al. (2010). Growth retardation, impaired triacylglycerol catabolism, hepatic steatosis, and lethal skin barrier defect in mice lacking comparative gene identification-58 (CGI-58). J. Biol. Chem. **285:** 7300–7311.

Slocombe, S.P., Cornah, J., Pinfield-Wells, H., Soady, K., Zhang, Q., Gilday, A., Dyer, J.M., and Graham, I.A. (2009). Oil accumulation in leaves directed by modification of fatty acid breakdown and lipid synthesis pathways. Plant Biotechnol. J. **7:** 694–703.

Strader, L.C., Wheeler, D.L., Christensen, S.E., Berens, J.C., Cohen, J.D., Rampey, R.A., and Bartel, B. (2011). Multiple facets of *Arabidopsis* seedling development require indole-3-butyric acid-derived auxin. Plant Cell **23:** 984–999.

Subramanian, V., Rothenberg, A., Gomez, C., Cohen, A.W., Garcia, A., Bhattacharyya, S., Shapiro, L., Dolios, G., Wang, R., Lisanti, M.P., and Brasaemle, D.L. (2004). Perilipin A mediates the reversible binding of CGI-58 to lipid droplets in 3T3-L1 adipocytes. J. Biol. Chem. **279:** 42062–42071.

Theodoulou, F.L., Job, K., Slocombe, S.P., Footitt, S., Holdsworth, M., Baker, A., Larson, T.R., and Graham, I.A. (2005). Jasmonic acid levels are reduced in COMATOSE ATP-binding cassette transporter mutants. Implications for transport of jasmonate precursors into peroxisomes. Plant Physiol. **137:** 835–840.

Yamaguchi, T., Omatsu, N., Matsushita, S., and Osumi, T. (2004). CGI-58 interacts with perilipin and is localized to lipid droplets. Possible involvement of CGI-58 mislocalization in Chanarin-Dorfman syndrome. J. Biol. Chem. **279:** 30490–30497.

Yamaguchi, T., Omatsu, N., Morimoto, E., Nakashima, H., Ueno, K., Tanaka, T., Satouchi, K., Hirose, F., and Osumi, T. (2007). CGI-58 facilitates lipolysis on lipid droplets but is not involved in the vesiculation of lipid droplets caused by hormonal stimulation. J. Lipid Res. **48:** 1078–1089.

Zolman, B.K., Silva, I.D., and Bartel, B. (2001). The *Arabidopsis pxa1* mutant is defective in an ATP-binding cassette transporter-like protein required for peroxisomal fatty acid β-oxidation. Plant Physiol. **127:** 1266–1278.

The α/β Hydrolase CGI-58 and Peroxisomal Transport Protein PXA1 Coregulate Lipid Homeostasis and Signaling in *Arabidopsis*

Sunjung Park, Satinder K. Gidda, Christopher N. James, Patrick J. Horn, Nicholas Khuu, Damien C. Seay, Jantana Keereetaweep, Kent D. Chapman, Robert T. Mullen and John M. Dyer

Plant Cell 2013;25;1726-1739; originally published online May 10, 2013;
DOI 10.1105/tpc.113.111898